# Topography-based Fuzzy Assessment of Runoff Area with 3D Spatial Relations *

Clément Iphar
Université Paris-Saclay, CEA, List, F-91120, Palaiseau, France
clement.iphar@cea.fr

Laurence Boudet
Université Paris-Saclay, CEA, List, F-91120, Palaiseau, France
laurence.boudet@cea.fr

Jean-Philippe Poli
Université Paris-Saclay, CEA, List, F-91120, Palaiseau, France
jean-philippe.poli@cea.fr

**Abstract**

Fuzzy logic has been successfully used in various crisis management systems. In such systems, the geographical aspect is usually very important and relies on Geographical Information Systems. Most of the approaches are focused on 2D information. In this paper, we use the fuzzy morpho-mathematics framework to define new relations to reason on the topography with a digital terrain model. In particular, we focus on the characterisation of the line of greatest dip. Without loss of generality, we then illustrate those relations on a case of runoff from a building and a terrain.

Fuzzy morpho-mathematics; topographic fuzzy reasoning; Geographical reasoning; topographic fuzzy relations; Crisis management

## 1 Introduction

Fuzzy logic has been successfully applied to crisis management [1, 2] thanks to its ability to deal with the vagueness of the involved knowledge and the uncertainty of the events. Some systems are directly connected to a Geographical Information System (GIS) [3,4] to enhance the reasoning on spatial objects that is often needed in such scenarios. These spatial decision support systems use

*This work is part of the ResponDrone project, which is funded by the European Union's H2020 Research and Innovation Program under Grant Agreement No. 833717.

either GIS to visualise information [5], to gather attributes and fuzzify them, or to get 2D objects and reason vaguely on them [6].

There are multiple ways to represent and assess spatial relations in fuzzy logic. In [7], the authors define topological and directional relations, adapting Allen's relations to spatial objects. They use an abstract spatial graph, a data structure that maintains all necessary information. Schockaert *et al.* [8] adapt region connection calculus to fuzzy logic, defining topological relations between vague regions. In [9], the authors model imprecise or uncertain regions using triangulated irregular networks. Finally, Bloch *et al.* [10] propose the Fuzzy Mathematical Morphology framework, which allows assessing both topological and directional relations, based on the fuzzification of two base operations: the dilation and the erosion.

Nevertheless, most of these approaches reason on 2D objects only [11,12]. In some cases, it is important to consider the elevation to handle the topography of a terrain. In particular, and without loss of generality, it is the case of liquid runoff. Liquid runoff occurs when there is more liquid than the land can absorb or when the liquid cannot be absorbed by the land. For given types of crises, like flooding or industrial liquid leaks, it is important to determine the areas that may be impacted.

In this article, we propose a new approach to reason on a Digital Terrain Model (DTM), based on Fuzzy Mathematical Morphology framework, which is seamlessly applicable on higher dimension than 2D. 3D applications have been documented in the medical domain [13], but they lack applications in the domain of geographical relations. We define relations that are able to define the areas that are impacted by runoff, without simulation or fluid mechanics insights. The idea is to have a compositional approach based on three relations: a directional relation (that needs the computation of the direction of greatest dip), a proximity one and one linked to the ground surface. We illustrate these reasoning abilities, without loss of generality, on a toxic liquid runoff from a building and a water runoff from a real historical site in Corsica.

This paper is organised as follows. Section 2 gives an overview of the approach to compute the fuzzy runoff area. Sections 3 to 5 give more details about the different formalisations. We then present the computation of the fuzzy runoff area and illustrate it on concrete examples in section 6 and draw some conclusions.

## 2 General approach to the computation of a fuzzy runoff area

In this paper, we consider any geographic feature of interest (a building, an area, ...) that can be represented by a spatial fuzzy set, a DTM of any kind, and we aim at computing the fuzzy set that is the outcome of a runoff from the original object of interest (represented as a fuzzy set), along the local lines of greatest dip of the DTM.

To achieve this, it is first necessary to define 2D and 3D structuring elements and eventually fuzzy landscapes for the spatial relations that are of particular interest for this runoff computation. First, the relation "*In the direction of*" with any azimuth angle has to be defined and computed, then associated with the elementary spatial relation "*Near*". Since the computation is performed on a DTM, it is further necessary to compute the local direction of the line of greatest dip at each point of interest across the landscape, therefore the algorithm required for successive points of the runoff from one given point has to be implemented. The DTM itself allows us to generate a fuzzy set for the spatial relation "*At ground level*" as we want to narrow down our outcome fuzzy set to the areas of $\mathbb{R}^3$ where most actual human activity takes place.

Eventually, when putting together the set of computed runoff points and the conjunction of the three spatial relations "*Near, at the ground level, in the direction of the greatest dip*", the final fuzzy set is computed, representing the most probable path followed by a runoff, thus showing the locations of interest for first responders.

# 3 Definition of a geographic direction as a fuzzy landscape

Following the definition of fuzzy landscape for cardinal directions defined by [14], we extend this notion to any angle $G \in [0, 2\pi[$.

## 3.1 Definition of the Structuring Element

Let us denote by $\nu_G^P$ the structuring element of the spatial predicate "*In the direction G*" taking the set of parameters $P = \{\theta_1, \theta_2\}$, with $\theta_1$ being the lower cut angle and $\theta_2$ being the upper cut angle. Considering each point of the space $\mathbb{R}^3$, with East, North and elevation coordinates, the problem is reduced to East and North coordinates, since the membership score of a point does only depend on the azimuth angle and does not depend on the elevation angle.

Let us consider the point $X$ of coordinates $(E_X, N_X, z_X)$, and the origin of the structuring element $O$ of coordinates $(0, 0, 0)$. The bearing of vector **OX** with respect to the North is computed as $\omega_{OX} = atan2(E_X, N_X)$, where $atan2(x, y) = Arg(x + iy)$, with $i^2 = -1$.

We denote as $\Delta_X^G$ the angular difference between $\omega_{OX}$ and $G$ as seem from point $O$. By construction, $\Delta_X^G$ takes values in $[0, \pi]$. For the points of the space for which the angular difference to $G$ is inferior to the lower cut angle $\theta_1$, the membership score to the spatial predicate of interest is maximum. In addition, for the points of the space for which the angular difference to $G$ is superior to $\theta_2$, the membership score to the spatial predicate of interest is minimum. Any intermediate value will result in an intermediate membership score, which decreases as $\Delta_X^G$ increases, and following a trigonometric function. Here the choice of the trigonometric function is arbitrary, other functions (linear or not, continuous or not, as long as defined at all points) could be used.

$\forall X \in \mathbb{R}^3 \setminus O$,

$$\nu_G^P(O)(X) = \begin{cases} 1 & \text{if } \Delta_X^G \leq \theta_1 \\ \cos \frac{\Delta_X^G - \theta_1}{\theta_2 - \theta_1} & \text{if } \theta_1 < \Delta_X^G < \theta_2 \\ 0 & \text{if } \Delta_X^G \geq \theta_2 \end{cases} \tag{1}$$

By construction, $\theta_1 \leq \theta_2$ and it is expected that $\theta_2 \leq \frac{\pi}{2}$ to avoid getting positive membership values for points that are completely outside the range of coordinates in the desired direction. Two instances of this structuring element are shown in Figure 1. In this Figure, and in all Figures of this paper, membership values rank between 0 and 1, from white (lower membership scores) to black (higher membership scores).

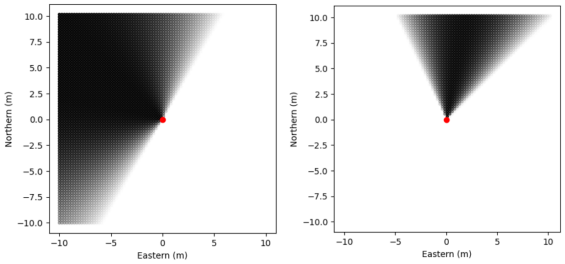


Figure 1: Two structuring elements $\nu_G$ representing the predicate "*In the direction G*". The red dot represents the centre of the structuring element. Set of parameters are as follow: left picture $G = 300°$, $\theta_1 = \pi/12$ and $\theta_2 = \pi/2$ ; right picture $G = 10°$, $\theta_1 = 0$ and $\theta_2 = \pi/5$

## 3.2 Fuzzy Dilation

The fuzzy dilation of an object B by the structuring element $\nu_G^P$ is presented here, as it will generate $\mu_G^P$ as an outcome, as shown in [13]. For the remaining of this paper, let us consider a fuzzy object of interest that we denote $B$ (the membership function being $\mu_B$), which is bi-dimensional in $\mathbb{R}^2$ problems and tri-dimensional in $\mathbb{R}^3$ problems. The membership value of the dilation of $B$ by $\nu_G^P$ at each point $X$ is denoted $\mu_G^P(B)(X)$ and computed as the supremum of the membership values of $\nu_G^P$ when applied to each point of $B$, or the local value of $\mu_B$, whichever is greater.

$\forall X \in \mathbb{R}^3$,

$$\mu_G^P(B)(X) = \perp\big(\mu_B(X), \sup_{b \in B}\big(\top(\mu_B(b), \nu_G^P(b)(X))\big)\big) \tag{2}$$

where $\top(\cdot,\cdot)$ is a t-norm and $\perp(\cdot,\cdot)$ is a t-conorm. Figure 2 shows the dilation of objects (in red) by the two structuring elements shown in Figure 1.

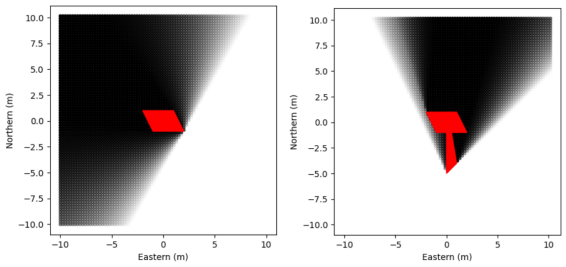


Figure 2: Fuzzy landscape of two objects (crisp in this example) dilated by $\nu_G$. Set of parameters are as follow: left picture $G = 300°$, $\theta_1 = \pi/12$ and $\theta_2 = \pi/2$; right picture $G = 10°$, $\theta_1 = 0$ and $\theta_2 = \pi/5$

### 3.3 Spatial Proximity Predicate

On top of the general consideration towards the direction, a consideration on the distance to the object can be considered, leading to the use of both "*near*" and "*In the direction of G*" and thus creating the predicate "*Near, in the direction of G*". In this respect, we define an operator "*near*" that has a structuring element that we denote as $\nu_n^{P'}$, taking the set of parameters $P' = \{\delta_1, \delta_2\}$. Those parameters are $\delta_1$ which is the lower cut distance, or the greatest distance for which the membership score is 1 and $\delta_2$ which is the upper cut distance, or the smallest distance for which the membership score is 0. As one of the elementary spatial primitives, as defined in [15], its definition is kept as simple as possible, to be later combined with other spatial predicates.

Denoting $\mathcal{D}_E(O, X)$ as the Euclidean distance between $O$ and $X$, $\forall X \in \mathbb{R}^3$, $\delta_1 \geq 0$, $\delta_2 \geq \delta_1$

$$\nu_n^{P'}(O)(X) = \begin{cases} 1 & \text{if } \mathcal{D}_E(O,X) \leq \delta_1 \\ 1 - \frac{\mathcal{D}_E(O,X) - \delta_1}{\delta_2 - \delta_1} & \text{if } \delta_1 < \mathcal{D}_E(O,X) < \delta_2 \\ 0 & \text{if } \mathcal{D}_E(O,X) \geq \delta_2 \end{cases} \tag{3}$$

Figure 3 shows the membership function of $\nu_n^{P'}$ and a representation of the structuring element in the $(E, N)$, in the horizontal plane that is at $z = 0$. Please take into consideration that the structuring element is actually of spherical shape.

### 3.4 "Spatial proximity in a direction" Predicate

The novel approach of this paper consists in considering both spatial predicates of direction and proximity in one single structuring element applied to the object of interest. We are therefore using a t-norm as we aim at performing a fuzzy intersection between the two concepts, as we use the approach of [10] using t-norms and t-conorms as fuzzy intersection and fuzzy union. For the sake of simplicity and without loss of generality, the only t-norm that will be used in

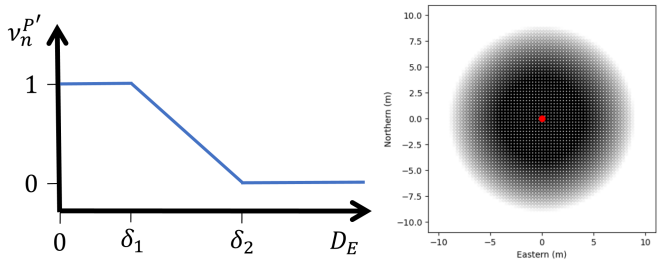


Figure 3: Left: membership function for the "*Near*" relation. Right: corresponding structuring element $\nu_n$ with $\delta_1 = 4$ and $\delta_2 = 9$

all illustrations of this paper is the product; however, it remains valid with any other t-norm that may be used to put the stress on specific behaviours.

Following the notations of Eq.1 and Eq.3, the membership value of the dilation of $B$ by $\nu_G^P$ and $\nu_n^{P'}$ at each point $x$ is denoted $\mu_{NG}^{P,P'}(B)(x)$ and computed as the supremum of the membership values of the t-norm operation on $\nu_G^P$ and $\nu_n^{P'}$ when applied to each point of the initial set. We denote the resulting structuring element $\nu_{NG}$ and it is computed in each point $X$ of $\mathbb{R}^3$ from any point $b$ of $B$ as

$$\nu_{NG}^{P,P'}(b)(X) = \top(\nu_G^P(b)(X), \nu_n^{P'}(b)(X)) \tag{4}$$

where $\top(\cdot,\cdot)$ is a t-norm. Then we compute $\mu_{NG}^{P,P'}$ as, $\quad \forall X \in \mathbb{R}^3$,

$$\mu_{NG}^{P,P'}(B)(X) = \bot\big(\mu_B(X), \sup_{b\in B}\big(\top(\mu_B(b), \nu_{NG}^{P,P'}(b)(X))\big)\big) \tag{5}$$

where $\top(\cdot,\cdot)$ is a t-norm and $\bot(\cdot,\cdot)$ is a t-conorm.

Figure 4 shows the dilation of the same objects with the same parameters of Figure 2 but with the structuring element $\nu_{NG}$ instead of $\nu_G$

# 4 Computation of the direction of greatest dip

Let us consider a point of interest $X$ represented by a set of geographic coordinates $(E_X, N_X, z_X)$ representing the East (or x-axis), North (or y-axis) and altitude. Let us consider a DTM, consisting of nodes describing the evolution of the terrain in 3D, on any network, in the general case a Triangulated Irregular Network. However, in this paper, we use a regular East and North grid, with an altitude value for each node, implemented in such a way that it is applicable to any network. More precisely, we use the DTM of the French National Institute of Geographic and Forest information (IGN), freely available online[1], with a grid step of 5 meters in both East and North directions, the coordinates are

[1] https://geoservices.ign.fr

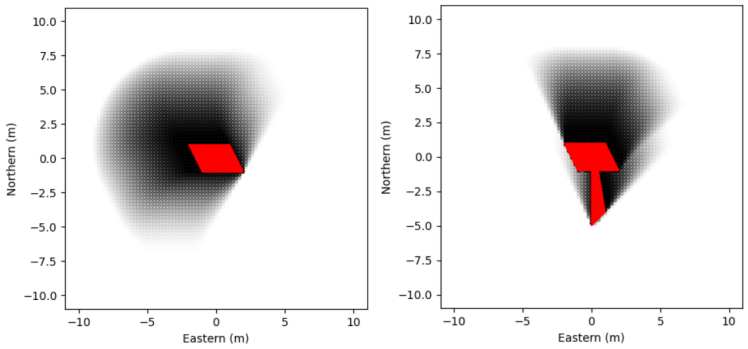


Figure 4: The same objects of Figure 2 dilated by $\nu_{NG}$ with the same sets of parameters, adding $\delta_1 = 2$ and $\delta_2 = 7$ for both pictures, considered in the plane of interest ($z = 0$)

following the French Lambert92 system and altitudes are expressed in meters with a centimetric precision in the IGN78 altimetric system.

Let us consider that such a DTM represents the surface of the Earth and thus can be divided in triangular sections (to create either Voronoi diagram), so that each point of the surface is part of the triangle defined by its three surrounding points. Let us denote those points as $I$, $J$ and $K$, of coordinates $(E_I, N_I, z_I)$, $(E_J, N_J, z_J)$ and $(E_K, N_K, z_K)$ respectively.

In the frame of the determination of the line of dip at point $X$, we compute the equation of the plane of the surface generated by those three vertexes. Let us compute the plane as $a \cdot E + b \cdot N + c \cdot z + d = 0$, taking generating vectors $V_1 = J - I = (E_J - E_I, N_J - N_I, z_J - z_I)$ and $V_2 = K - I = (E_K - E_I, N_K - N_I, z_K - z_I)$. We compute $n$ as $V_1 \times V_2$, then by definition $a = n_E$, $b = n_N$ and $c = n_z$, and $d$ is determined from any of the $I$, $J$ and $K$ points for which the three coordinates are known by solving the equation.

Altitudes on the plane, including the one of $X$ can be computed as

$$z = -\frac{1}{n_z} \cdot (n_E \cdot E + n_N \cdot N + d) \tag{6}$$

and the line of greatest dip $\theta$ is computed as

$$\begin{array}{ll} \tan(\theta) = \frac{n_E}{n_N} & \text{if } n_N \neq 0 \\ \theta = \frac{\pi}{2} & \text{if } n_N = 0 \text{ and } n_E > 0 \\ \theta = -\frac{\pi}{2} & \text{if } n_N = 0 \text{ and } n_E < 0 \\ \text{undefined} & \text{if } n_N = 0 \text{ and } n_E = 0 \end{array} \tag{7}$$

We deem this last case as highly unlikely, since it would require that all three points are at the exact same centimetric altitude, however would this case take place, the direction of the line of greatest dip would not be computed, as no favoured direction would exist.

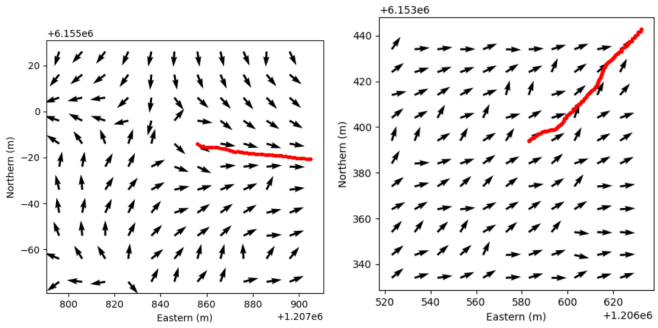


Figure 5: Two fields of lines of greatest dip, with the line of greatest dip showing a runoff from the centre of the field is shown in red.

Procedure 1 shows the iterative process that leads to the generation of the trajectory of the runoff, under the form of a track, as it can be shown in Figure 5. Major parameters of the algorithm are $E$, the Eastern coordinate (or longitude), $N$, the Northern coordinate (or latitude), $\Lambda$, a digital terrain model, constituted by a series of Eastern, Northern and altitude coordinates $(E_\Lambda, N_\Lambda, z_\Lambda)$. In addition, there are some minor parameters of the algorithm: $s$, a numerical value representing the distance of the step forward for the computation of the coordinates for the next iteration, $\Xi$, a bounding box for both coordinates, out of which we want the computation to stop and $m$, an integer standing for the maximum number of iterations before stopping the computation even if the points are still within $\Xi$. The output of the algorithm is $R_{E,N,\Lambda,s,\Xi,M}$, that we denote $R_{E,N}$ for the sake of simplicity, and is a set of 3D points.

**Procedure 1** Compute the runoff track

**Input:** $E, N, \Lambda, s, \Xi, m$
**Output:** $R_{E,N}$
  $R_{E,N} \leftarrow [\,]$ {Output array is created empty}
  $e \leftarrow E$ {Variable initialisation}
  $n \leftarrow N$ {Variable initialisation}
  $k \leftarrow 0$ {Counter initialised}
  **while** $(e, n) \in \Xi$ **and** $k < m$ **do**
    $k \leftarrow k + 1$ {Counter incremented}
    $z = f_1(e, n, \Lambda)$ {cf. Eq.6}
    $\theta = f_2(e, n, \Lambda)$ {cf. Eq.7, unchanged if undefined}
    $R_{E,N} \leftarrow R_{E,N} \bigcup \{e, n, z\}$ {Point is added to output}
    $e \leftarrow e + s \cdot \sin(\theta)$ {Next point East coord. is computed}
    $n \leftarrow n + s \cdot \cos(\theta)$ {Next point North coord. is computed}
  **end while**

# 5 Definition of the ground level as a fuzzy landscape

In this section, we are interested in creating a fuzzy landscape for the determination of the ground level, *i.e.* the area of space that is just above the ground. This landscape covers the whole area of interest, and rather than considering the geometrical distance between the surface (represented by a collection of polygons) and the point of interest, we consider the vertical distance between the point and the surface, as it takes into consideration the only direction that matters in terms of height: the z-axis.

## 5.1 Membership Score

Let us consider a point $X$ of coordinates $(E_X, N_X, z_X)$ in $\mathbb{R}^3$. Let us compute $z_0$, the altitude according to the DTM of interest, computed as shown in Eq.6. Let us define $\Delta z = z_X - z_0$ as the height above the ground at the point of interest. Figure 6 shows such membership function, as defined by Eq.8.

$\forall X \in \mathbb{R}^3, \tau_1 \geq 0, \tau_2 \geq \tau_1,$

$$\mu(\Delta z) = \begin{cases} 0 & \text{if } \Delta z < 0 \\ 1 & \text{if } 0 \leq \Delta z \leq \tau_1 \\ 1 - \frac{\Delta z - \tau_1}{\tau_2 - \tau_1} & \text{if } \tau_1 < \Delta z < \tau_2 \\ 0 & \text{if } \Delta z \geq \tau_2 \end{cases} \tag{8}$$

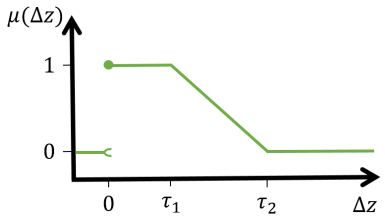


Figure 6: Membership function "*at ground level*" with respect of the computed value of $\Delta_z$ for any point $X$ of $\mathbb{R}^3$

## 5.2 Application to a Digital Terrain Model

We then apply the simple membership function shown in Figure 6 to the whole surface of the DTM, by applying the $\mu(\Delta z)$ function to all points of the terrain within the boundary box of interest, according to the local height at each point. The resulting 3D fuzzy set is denoted $\mu_T$. An illustration of the terrain and of the resulting fuzzy set computed with the set of parameters $\tau_1 = 1\ m$ and $\tau_2 = 3\ m$ is shown in Figure 7.

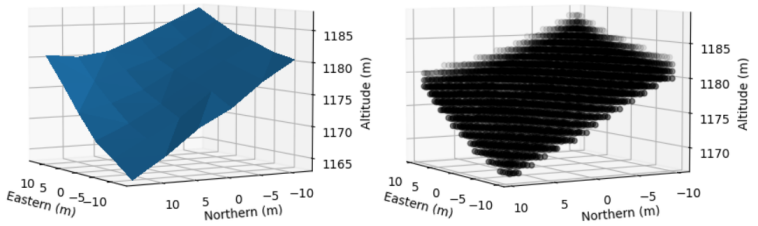


Figure 7: Left: 20m × 20m excerpt of the DTM. Right: Fuzzy set for the spatial relation "*At Ground Level*" on the same DTM area. Centered on $E = 1201690$, $N = 6147769$, for the sake of the example

# 6 Fuzzy runoff area computation and application to a building

We contextualise an application around a spill of liquid from a building. The spatial extent of the building, denoted $B$, is known, as well as the local terrain. The computation process takes three steps, the first one being the computation of all runoff tracks from all the points of the object, defined as a fuzzy set denoted $\mu_R$. The second step consists of the dilation of $\mu_R$ by $\nu_{NG}$, the structuring element considered at the point of interest. Last, the third step consists to take into consideration the ground surface $\mu_T$ as computed in Section 5. In this section, all figures are shown with the following set of parameters: $P = [\pi/12, \pi/4]$, $P' = [5, 20]$, and when necessary $\tau_1 = 1$ and $\tau_2 = 3$.

## 6.1 Computation of the Runoff Area

When $B$ is fuzzy, the collection of runoff tracks, denoted $\mu_R$, is a fuzzy set, the membership score for each point of the runoff being determined from the membership score of the point of $B$ from which it originated. We define the resulting fuzzy set $\mu_R$ as the fuzzy union of all runoff tracks from all points of the object $B$. We compute this set in several steps. First, we denote all points originating from $b^{th}$ element of $B$ as the fuzzy set $\mu_{R_b}$

$$\mu_{R_b} = \{\big(X, \mu_B(b)\big) | X \in R_{E_b,N_b}\} \tag{9}$$

taking $\mu_B(b)$ as membership value of $B$ at point $b$ and where $R_{E_b,N_b}$ is the set of points computed by Procedure 1 given that $E_b$ and $N_b$ are the coordinates of point $b$.

Then, we compute $\mu_R$ is such a way that

$$\mu_R = \underset{b \in B}{\cup} \mu_{R_b} \tag{10}$$

where $\cup$ is the fuzzy union of two fuzzy sets such that $\forall b, b' \in B,\ b \neq b'$,

$$\mu_{R_b} \cup \mu_{R_{b'}} = \{\big(X, \max(\mu_{R_b}(X), \mu_{R_{b'}}(X))\big) | \\ X \in R_{E_b,N_b} \cup R_{E_{b'},N_{b'}}\}. \quad (11)$$

## 6.2 Generation of the Runoff Area Dilation

According to Eq. 5, the raw runoff fuzzy set is dilated by $\nu_{NG}$ and the resulting set is denoted $\mu_B^{NG}$, and computed $\forall X \in \mathbb{R}^3$ as

$$\mu_B^{NG}(X) = \perp\big(\mu_R(X), \sup_{b \in B}\big(\top(\mu_R(b), \nu_{NG}(b)(X))\big)\big) \quad (12)$$

where $\perp(\cdot,\cdot)$ is a t-conorm and $\top(\cdot,\cdot)$ is a t-norm.

## 6.3 Consideration of the Ground Level

The last step consists in performing the intersection of $\mu_B^{NG}$ and $\mu_T$. The resulting fuzzy set, the fuzzy runoff area, denoted $\mu_B^*$, is computed as, $\forall X \in \mathbb{R}^3$,

$$\mu_B^*(X) = \top(\mu_B^{NG}(X), \mu_T(X)) \quad (13)$$

where $\top(\cdot,\cdot)$ is a t-norm. Figure 8 shows the outcome of the computation for the same runoff in both 2D and 3D visual representation.

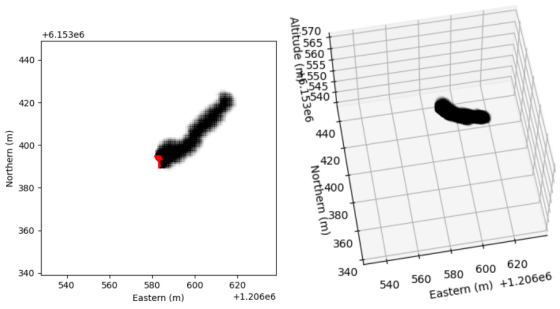


Figure 8: Two-dimensional from above (left) and three-dimensional (right) representations of the same runoff area

This method allows highlighting the cases in which various parts of the initial set (the building) will lead to distinct runoff areas, due to the local topography. While Figure 8 shows a rather homogeneous runoff direction, Figure 9 shows two different runoff areas that are constituted by a plurality of branches.

## 6.4 Application to an Actual Building

In this section, we want to show an application of the method not to a polygon figuring a building, such as shown in section 6.3 but to an actual building,

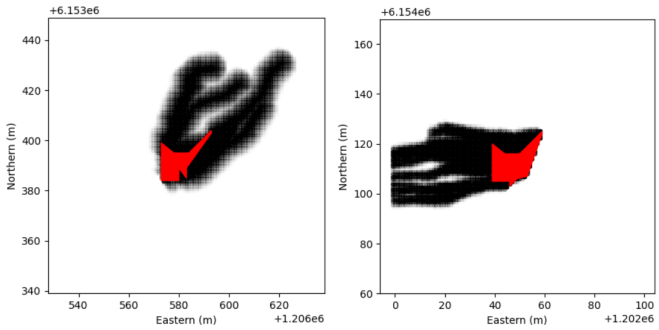


Figure 9: Examples of runoff from crisps polygons, with various shapes and from different points on the DTM

extracted from an *ad hoc* database. To this end, we have selected the Corte castle, located in Corte, France, and extracted its geometry using publicly available data from Open Street Map[2]. This analysis could be performed with any building for which the geometry is known, but this castle, located at the top of a rocky peak, displays complex topographic surroundings, and the generation of a runoff map would be advantageous to first responders. Figure 10 shows a picture of the castle, to underline its topographic features.

Figure 10: View of the Corte castle (from South)

The outcome of the computation is shown in Figure 11, showing for instance the discharge ways of water in the event of intense rainfalls.

# 7 Conclusion

In this paper, we use the fuzzy morphomathematics framework to define three-dimensional topographic relations involving the line of greatest dip and the

[2]https://www.openstreetmap.org/

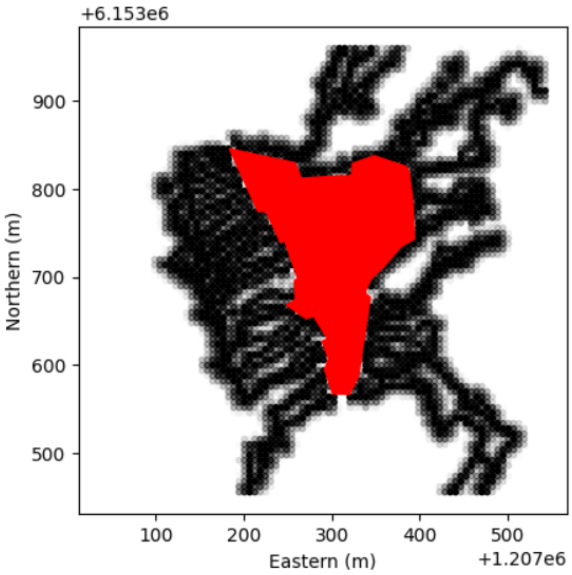


Figure 11: Runoff area from the Corte castle

notion of ground level. The use of morphomathematics was motivated by its adaptability to 3D relations. Those relations have been defined with our own structuring elements, through which fuzzy objects are dilated. We applied such relations to the computation of a runoff area, the outcome of which being a fuzzy set computed upon a local DTM, providing a clearer understanding of the scene to first responders.

We exemplify this framework with a runoff from the castle of Corte, France. Future work will focus on the definition of further relations to develop a broader set of topography-based relations to reason on fuzzy geographical features in 3D.

# References

[1] A. Alnahhas and B. Alkhatib, "Decision support system for crisis management using temporal fuzzy logic," in *2012 6th International Conference on Application of Information and Communication Technologies (AICT)*, 2012, pp. 1–5.

[2] X. Jia, G. Morel, H. Martell-Flore, F. Hissel, and J.-L. Batoz, "Fuzzy logic based decision support for mass evacuations of cities prone to coastal or river floods," *Environmental Modelling & Software*, vol. 85, pp. 1–10, 2016.

[3] F. Di Martino, I. Perfiljeva, S. Sessa, and S. Senatore, "Fuzzy methods and approximate reasoning in geographical information systems," *Advances in Fuzzy Systems*, vol. 2014, 2014.

[4] L. Boudet, J. P. Poli, L. P. Bergé, and M. Rodriguez, "Situational assessment of wildfires: a fuzzy spatial approach," in *2020 IEEE 32nd International Conference on Tools with Artificial Intelligence (ICTAI)*, 2020, pp. 1180–1185.

[5] A. Calzada, J. Liu, H. Wang, and A. Kashyap, "A gis-based spatial decision support tool based on extended belief rule-based inference methodology," in *Proceedings of the Fourth International Workshop on Knowledge Discovery, Knowledge Management and Decision Support*. Atlantis Press, 2013/10, pp. 388–395.

[6] A. Dilo, R. A. de By, and A. Stein, "A system of types and operators for handling vague spatial objects," *Int. J. Geogr. Inf. Sci.*, vol. 21, no. 4, p. 397–426, Jan. 2007.

[7] M. A. Cobb and F. E. Petry, "Modeling spatial relationships within a fuzzy framework," *Journal of the American Society for Information Science*, vol. 49, no. 3, pp. 253–266, 1998.

[8] S. Schockaert, M. D. Cock, and E. Kerre, *Reasoning About Fuzzy Temporal and Spatial Information from the Web*. USA: World Scientific Publishing Co., Inc., 2010.

[9] J. Verstraete, G. De Tre, A. Hallez, and R. De Caluwe, "Using tin-based structures for the modelling of fuzzy gis objects in a database," *International Journal of Uncertainty, Fuzziness and Knowledge-Based Systems*, vol. 15, pp. 1–20 (suppl.), 2007.

[10] I. Bloch and H. Maitre, "Fuzzy mathematical morphologies: A comparative study," *Pattern Recognition*, vol. 28, no. 9, pp. 1341–1387, 1995.

[11] C. Leroux, H. Jones, L. Pichon, S. Guillaume, J. Lamour, J. Taylor, O. Naud, T. Crestey, J.-L. Lablee, and B. Tisseyre, "GeoFIS: An open source, decision-support tool for precision agriculture data," *Agriculture*, vol. 8, no. 6, 2018.

[12] A. Chaves Carniel, M. Schneider, and R. R. Ciferri, "FIFUS: A rule-based fuzzy inference model for fuzzy spatial objects in spatial databases and GIS," in *Proceedings of the 23rd SIGSPATIAL International Conference on Advances in Geographic Information Systems*, 2015.

[13] I. Bloch, "Fuzzy relative position between objects in image processing: a morphological approach," *IEEE Transactions on Pattern Analysis and Machine Intelligence*, vol. 21, no. 7, pp. 657–664, 1999.

[14] C. Hudelot, J. Atif, and I. Bloch, "Fuzzy spatial relation ontology for image interpretation," *Fuzzy Sets and Systems*, vol. 159, pp. 1929–1951, 2008.

[15] J. Freeman, "The modelling of spatial relations," *Computer Graphics and Image Processing*, vol. 4, no. 2, pp. 156–171, 1975.